

## Research Article

# Vehicle Load Spectrum and Fatigue Vehicle Model of a Long-Span Concrete-Filled Steel Tube (CFST) Arch Bridge Based on Measured Data of Weight-In-Motion System

Luming Deng  and Yulin Deng 

*Department of Road and Bridge Engineering, School of Transportation and Logistics Engineering, Wuhan University of Technology, Wuhan 430063, China*

Correspondence should be addressed to Yulin Deng; [dengyulin@whut.edu.cn](mailto:dengyulin@whut.edu.cn)

Received 4 August 2022; Revised 20 September 2022; Accepted 7 October 2022; Published 22 October 2022

Academic Editor: Jian Lin Liu

Copyright © 2022 Luming Deng and Yulin Deng. This is an open access article distributed under the Creative Commons Attribution License, which permits unrestricted use, distribution, and reproduction in any medium, provided the original work is properly cited.

Highway traffic load, speed, and volume have been increasing continuously over the years. Because of its special structural form, the fatigue problem of a long-span concrete-filled steel tube arch bridge becomes more and more serious. To research the vehicle load spectrum and fatigue vehicle model of a long-span concrete-filled steel tubular arch bridge, the traffic data of the arch bridge were collected using the weight-in-motion system. The vehicle type and vehicle load in the actual traffic flow have strong stochastic characteristics, which cannot be directly applied. Therefore, according to the measured data, 10 representative models are proposed to facilitate the classification and screening of vehicle data. The wheelbase, mass, axle load, and overload data of the representative vehicle types were analysed, and the axle load distribution characteristics of vehicles in different lanes were studied. It is found that the vehicle load is not uniformly distributed in different lanes but concentrated in one lane. Moreover, a vehicle load spectrum for the fatigue assessment of the long-span concrete-filled steel tubular arch bridge is proposed. Based on the fatigue damage equivalence principle, a fatigue vehicle model and a simplified fatigue vehicle model of bridge heavy-duty vehicles are proposed. Compared with the model in the AASHTO specification, it is found that the weight of the local fatigue vehicle load model is 15.1 t heavier than the vehicle model given in the specification. This study could be further referenced in bridge-fatigue life prediction, management and maintenance, etc.

## 1. Introduction

In recent years, with the continuous increase in highway traffic flow, the fatigue problem of highway bridges has become increasingly significant. The structure of a long-span concrete-filled steel tube (CFST) arch bridge is complex, and the service environment is unsuitable. Generally, there are three main types of fatigue load spectra [1–3]: (a) a heavy vehicle with a static strength design standard live load, the result of which may be conservative; (b) the spectrum of the frequency value of a vehicle load, which is apparent in various representative models that are obtained through traffic surveys in daily operation [4]; and (c) the standard fatigue vehicle, derived by simplifying the vehicle load spectrum obtained by the second method [5].

Laman and Nowak believed that the vehicle load spectrum acting on a bridge had distinct regional characteristics, and the vehicle load intensity was greater in industrial developed areas. Moreover, the traffic load is not evenly distributed on each lane, and some lanes bear most of the traffic load [6]. Cohen et al.'s research shows that the ultimate load capacity of vehicles is increasing year by year, and some truck models in fatigue design specifications are no longer applicable to the current driving environment [7]. Obrien et al., based on extensive weight-in-motion measurements from two European sites, show the sensitivity of the characteristic traffic load effects to the fitting process. A semi-parametric fitting method is proposed, that is, direct use of the measured histogram where there are sufficient data for this to be reliable and parametric fitting to a statistical

distribution in the tail region where there are less data [8]. Zhao and Tabatabai proposed the maximum allowable truck model based on the weight-in-motion system, which in turn is based on the vehicle model with maximum damage determined by the loading analysis of 5% heavy trucks in the traffic flow. He suggested that a five-axle vehicle should be adopted as the maximum allowable truck model in Wisconsin [9]. Fiorillo and Ghosn analysed the traffic flow data collected by the weight-in-motion system on American highways and found that the increasing number of overloaded vehicles accelerated the fatigue loss of highway bridges, leading to high maintenance and reinforcement costs [10]. Leahy et al. investigated the truck data of 17 highways in 16 states of the United States, compared the loading results of the HL-93 fatigue vehicle model, and proposed a modified vehicle model [11]. Han et al. conducted a comparative study on the truck-overload data collected by substandard fatigue vehicles and a dynamic heavy system. The results showed that 80% of the overloaded vehicles had a mass of 80–130 t, and six-axle overloaded vehicles accounted for 97.86% of the total number of overloaded vehicles [12]. Yongtao et al. pointed out that China has a large territory and cannot directly apply the European and American fatigue car model specifications. According to a large number of road and bridge traffic vehicle load measured data, the standard fatigue vehicle of each province is combined, and a unified standard fatigue vehicle model is adopted for design [13]. Lan et al. used the monitoring data obtained from the bridge health monitoring system to make statistics on the probability distribution model and extreme value distribution of the total vehicle weight. By combining the fatigue load spectrum with the prediction model based on traffic volume, a load model bridge was provided to estimate the fatigue damage evolution [14]. Lu et al. used a probabilistic model of real vehicle loads as a basis for fatigue stress spectra to evaluate the reliability of bridges and develop fatigue limit state functions that consider traffic growth factors and vehicle weight. A steel bridge was taken as an example to illustrate the feasibility of the proposed stochastic fatigue vehicle load model [15]. However, due to China's vast territory, vehicle load spectra vary in different regions; therefore, it is difficult to propose a unified fatigue load model for steel bridges. In addition, due to issues related to regional traffic organization and urban planning, some bridges carry heavy-truck traffic and have a high proportion of overloaded vehicles, thus forming a vehicle load spectrum type that is significantly different from the proposed code. Zhang et al. used the traffic flow data generated by the program and established the fatigue vehicle model to analyze the influence of vehicle load on the fatigue life of the derrick of arch bridges in southwest China [16]. Chen et al. studied the traffic flow parameters of various vehicles based on fatigue data obtained from the long-term structural health monitoring system of a composite arch bridge. Representative vehicle types and vehicle characteristic data are determined. Finally, the fatigue performance of various derrick is analysed [17]. Sun et al. found that repeated action of vehicle load was the main type of fatigue failure of suspenders of an arch bridge. Through 24

hours of traffic flow investigation, the traffic load spectrum was established, and the fatigue reliability analysis model based on the cumulative damage model was proposed [18]. The traffic load on the CFST arch bridge may lead to premature cracks in the suspender and other components, which will affect the service state and durability of the bridge [19, 20]. The actual vehicle load on highways often exceeds the design load, which not only causes irreversible damage to bridge components but also threatens highway safety and bridge operation. Owing to the different operating environments in different places, the load levels of bridges on different lanes, and even on the same line, are not the same [21].

To study the fatigue vehicle load model adapted to the local road conditions, based on the vehicle load data obtained from the dynamic weighing system, this paper conducts statistical analysis on the vehicles actually observed on the bridge, classifies and summarizes different vehicle load types, and obtains the fatigue vehicle model in line with the local driving conditions. Therefore, it is of great importance to develop a vehicle load spectrum and fatigue load model for long-span CFST arch bridges to improve the vehicle load spectrum of highway bridges and complement the fatigue load model used for the fatigue design and evaluation of suspenders and other components on long-span CFST arch bridges.

## 2. Vehicle Statistics of the Dynamic Load-Bearing System

The dynamic weighing system is located at the Beisheng bridge in Yangquan, Shanxi Province. The overall appearance of the bridge is shown in Figure 1. The long-span suspender arch bridge is a half-through CFST arch bridge spanning a deep ditch in a mountainous area with a main span of 260 m. The carriageway beam is a  $7.5 + 3 \times 9 + 9.85 + 8.15 + 19 \times 9 + 8.15 + 9.85 + 3 \times 9 + 7.5$  m reinforced concrete  $\pi$ -shaped beam. The elevation design of the bridge is depicted in Figure 2. The entire bridge adopts simple support first and then continuous construction technology. The layout of the bridge lanes is shown in Figure 3, and the management and maintenance unit in this area has established a dynamic weighing system to record the number of vehicles in the driving lane, vehicle speed, vehicle mass, axle load, axle number, wheelbase, and other parameters. These basic data can provide an important basis for the fatigue assessment of the bridge and can be used to estimate the service life of the bridge suspenders [22].

In this study, driving load data were recorded from the 1<sup>st</sup> to the 30<sup>th</sup> of September, 2019. The recorded data show that the daily average number of vehicles passing through the bridge is 11,394, as shown in Figure 4. The vehicles in the driving data are classified according to the number of axles, as shown in Figure 5. According to the statistics in the figure, two-axle vehicles account for the largest proportion of passing vehicles, with an average of 4,260 vehicles per day, and the vehicle load variability is large. The daily average number of freight cars with different axle numbers shows different characteristics. There are approximately two



FIGURE 1: Beisheng CFST arch bridge. (a) Arch bridge lane. (b) Overall state of an arch bridge.

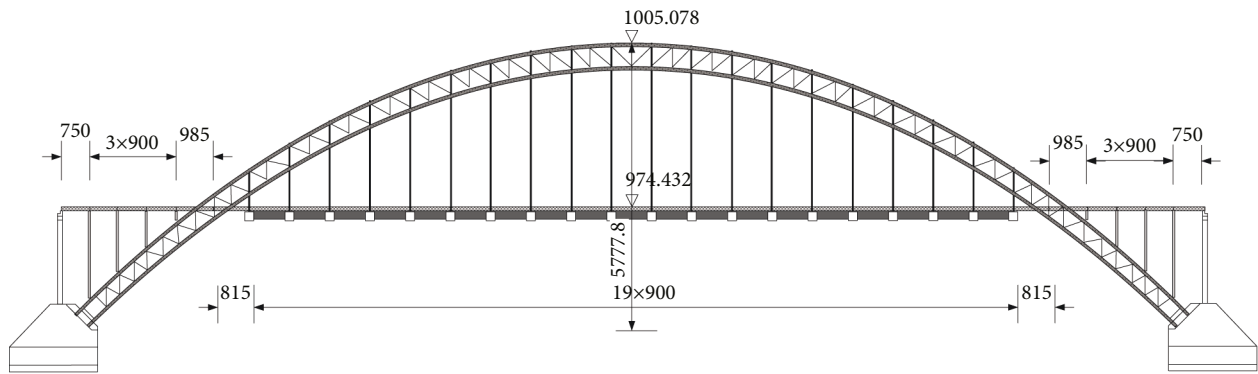


FIGURE 2: Bridge elevation structure drawing (unit: cm).

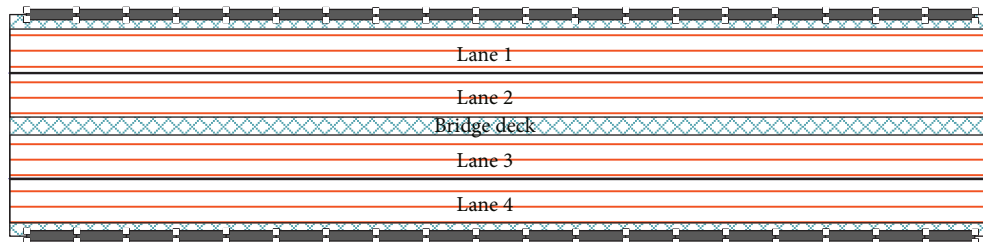


FIGURE 3: Bridge lane number.

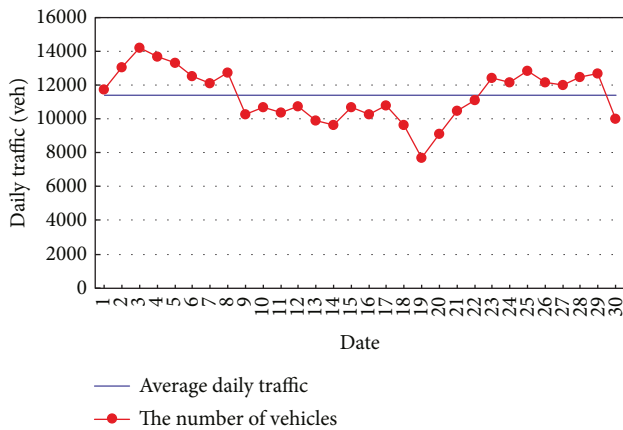


FIGURE 4: Daily traffic volume.

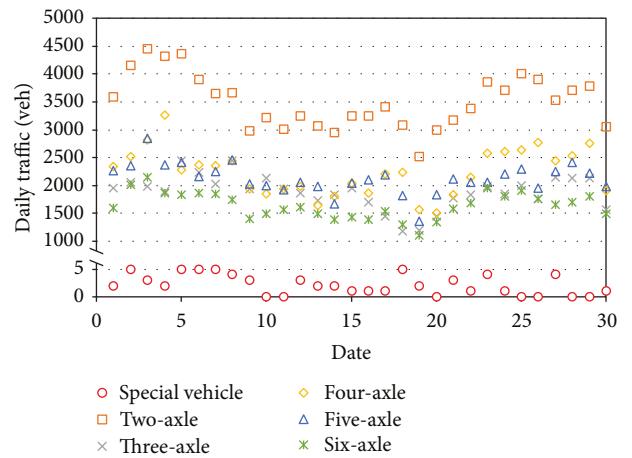


FIGURE 5: Daily traffic volumes of different numbers of axles.

vehicles with seven axles and above, and there are other special vehicles passing every day. The traffic frequency on the bridge is extremely small, and such vehicles do not reach their full-load capacity. Therefore, the damage caused by such vehicles to the bridge can be neglected. Three representative days are selected in Figure 6 according to the time-sharing statistics of traffic volume, and it can be observed from the figure that after 8:00 a.m., the traffic volume increases sharply, whereas after 6:00 p.m., the traffic volume begins to stabilize; therefore, more attention should be paid to the latter period in bridge maintenance management.

The dynamic weighing system was used to obtain the daily driving quantity, total vehicle mass, wheelbase, and axle load corresponding to 24 types of vehicles, as listed in Table 1, where  $D_i$  is the mean value of the  $i$ -th wheelbase of the target vehicle,  $\sigma$  is the standard deviation corresponding to the  $i$ -th wheelbase of the target vehicle, and  $G$  and  $g$  represent the total vehicle weight and standard deviation of the target model, respectively. In this study, the counted vehicles are classified into representative models V1–V11 according to their wheelbase, as presented in Table 2, where  $A$  is the  $k$ -th equivalent axle load of the target vehicle. It can be seen from Table 1 that the variation in wheelbase is not large, and the maximum standard deviation of the wheelbases of individual vehicles, such as 5-axle type III vehicles, reached 3.7 m. However, due to the low frequency of occurrence, their overall impact on the sample is limited, and they can be classified into similar vehicles according to the wheelbase ratio. Compared with wheelbase, the variability of the total vehicle mass is larger. The average vehicle mass of vehicles with three or more axles is larger, and the daily traffic volume reached 9320. It can be seen that the traffic volume of trucks is large and the traffic proportion is high, which shows that the freight load borne by this bridge is heavy.

### 3. Parameter Analysis of Vehicle Load Spectrum

Strength and loading frequency are the main parameters of the vehicle load spectrum. In the study of fatigue load spectra, it is not sufficiently comprehensive to only consider the total vehicle weight as the applied load; the response characteristics of the structure to the vehicle load should also be considered [23]. When a long wheelbase truck passes through a bridge, the load transmitted to the boom may have multiple stress cycles. To study the fatigue load model more comprehensively, it is necessary to refine the vehicle load parameters according to the axle load and wheelbase. In addition, the lane distribution of the driving load should be considered for specific bridges [24].

**3.1. Wheelbase and Axle Number.** For the division of representative vehicle types, wheelbase is an important characteristic parameter of the vehicle load spectrum. The wheelbase of each representative vehicle type is taken as the weighted average of vehicle wheelbases classified under the same representative vehicle type, calculated as follows:

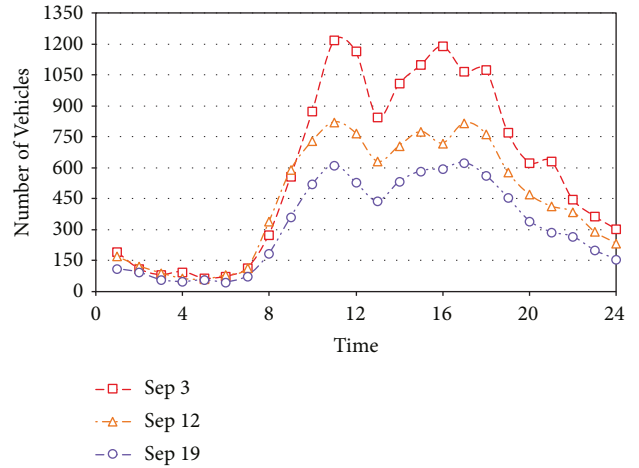


FIGURE 6: Time-sharing statistics of traffic flow.

$$L_i = \sum_{j=1}^n L_{ij}/n, \quad (1)$$

where  $L_i$  is the calculated  $i$ -th wheelbase of the representative vehicle,  $L_{ij}$  is the  $i$ -th wheelbase of the  $j$ -th car classified under the same representative vehicle type, and  $N$  is the total number of vehicles of this type of representative vehicle.

From Tables 1 and 2, it can be seen that the average vehicle mass of the V1 model is less than 3 t, and the daily average is more than 2521 veh, accounting for 21.4% of the total number of vehicles. Therefore, this vehicle model is considered to not cause bridge-fatigue damage and can be neglected in the fatigue load spectrum [6]. The daily average traffic volume of V2 and V3 axle cars is 2075 veh. The daily average traffic volume of V4 and V5 three-axle cars is 1742. The daily average traffic volume of V6 and V7 four-axle cars is 1181. The average daily traffic volume of V8 and V9 five-axle cars is 648. Because the average daily traffic volume of V9 models is relatively small, and because these models are representative in China, they are classified into one category. The average daily traffic volume of six-axle cars, namely V10 and V11, is 1531. If the wheelbase is approximately 1.3 m, the front and rear are considered to be adjacent. Three axles are defined as double axles (such as the rear two axles of a four-axle car), and three axles with front and rear adjacent wheelbases of approximately 1.3 m are defined as triple axles (such as the V8 and rear three axles of a six-axle car), such that the types of axle groups can be divided into single, double, and triple axles.

**3.2. Vehicle Mass.** The actual vehicle mass can directly reflect the load intensity and is an important parameter for the fatigue assessment of bridge suspenders [25]. According to the principle of fatigue damage equivalence, the equivalent vehicle mass is given as

$$W = \left( \sum_{j=1}^n f_j W_j^3 \right)^{1/3}, \quad (2)$$

TABLE 1: Vehicle data.

Type	Quantity	$D_1$ (m)	$d_1$ (m)	$D_2$ (m)	$d_2$ (m)	$D_3$ (m)	$d_3$ (m)	$D_4$ (m)	$d_4$ (m)	$D_5$ (m)	$d_5$ (m)	G (t)	$g$ (t)	Classification
Two-axle I	2521	1.6	0.1									2.3	1.2	v1
Two-axle II	654	2.9	0.2									4.7	1.5	v2
Two-axle III	218	3.2	0.2									9	2.7	
Two-axle IV	781	5.2	0.7									14	7.3	v3
Two-axle V	421	7.2	0.5									22	10.6	
Three-axle I	114	1.9	0.1	4.8	0.4							7.5	3.8	v4
Three-axle II	200	3.6	0.5	1.8	0.4							16	17.9	
Three-axle III	1037	5.4	0.8	1.4	1.9							28	11.6	
Three-axle IV	489	6.5	2.5	3.5	1.5	2.1						35	12.3	v5
Four-axle I	335	1.4	1.8	4.5	0.4	1.4	0					12.8	4.8	v6
Four-axle II	817	1.9	0.6	4.1	0.2	1.3	0.2					17	9	
Four-axle III	609	1.6	2.6	4.3	0.8	1.4	0.1					26	18.2	
Four-axle IV	760	3.5	3.3	10.8	2.4	1.3	0					35.4	22.2	v7
Four-axle V	408	4.1	2.6	7.8	1.1	2.9	0.3					45	15.6	
Five-axle I	622	1.3	4.1	4.6	2.4	1.3	0.2	1.3	0			15	6.7	V8
Five-axle II	37	2.1	3.2	5.1	3.7	8.4	2.2	1.3	0.2			28	13.5	
Five-axle III	13	4.2	2.9	1.4	0.2	8.8	4.8	1.4	0.1			35	16.4	V9
Five-axle IV	3	5.2	2.1	5	3.2	1.4	0.3	1.3	0			46	23.6	
Six-axle I	634	1.7	0.3	4.8	2.3	1.3	0.2	1.3	0.1	1.3	0	27	17.4	V10
Six-axle II	806	2.3	0.2	1.3	0.1	5.2	3.6	1.3	0.1	1.3	0	39	23.8	
Six-axle III	197	3.9	0.5	1.4	0.2	6.1	1.4	1.4	0.1	1.3	0.2	45	19.6	
Six-axle IV	45	3.2	0.8	1.4	0.2	9.5	7.3	1.3	0	1.3	0	53	22.7	V11
Six-axle V	126	1.8	0.2	2.6	0.1	8.2	1.7	1.3	0	1.3	0	68	25.2	

where  $W$  is the equivalent vehicle mass of a representative model,  $f_j$  is the relative frequency of the  $j$ -th car belonging to the representative model, that is, the frequency value of the  $j$ -th car in all statistical vehicles of this model, and  $W_j$  is the vehicle mass of the  $j$ -th car of the representative model.

When calculating the equivalent mass and equivalent axle load of statistical vehicles, the data of vehicles with a mass of less than 3 t were excluded [6]. Figure 7 shows that the total mass of the vehicle tended to increase with the increase in the number of vehicle axles. The minimum equivalent vehicle mass of the V2 model was 7.7 t, and the maximum equivalent vehicle mass of the V10 model was 64.5 t. The V9 model had only 24 veh, but the equivalent vehicle mass reached 63.1 t. Therefore, the influence of the V9 model on the bridge cannot be ignored. As can be seen from the statistical figure, the V2 model presents a single-peak skewness distribution, and the other types of vehicles present multi-peak distributions. The V3–V11 models are mainly trucks, the total mass of vehicles is affected by the quality of the goods they carry, and overloading often occurs. Therefore, there will be many peaks near the normal load and overload load ranges of the vehicle (Table 3).

**3.3. Axle Load.** The number of stress amplitude cycles is related to the number of vehicle axles. Therefore, a truck with a long wheelbase may generate multiple stress amplitudes during its travel. The  $i$ -th equivalent axle load of a

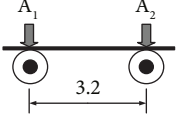
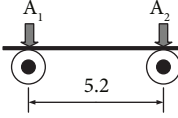
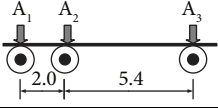
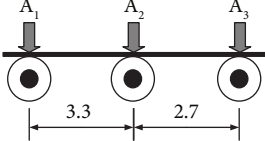
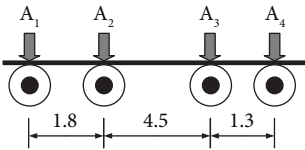
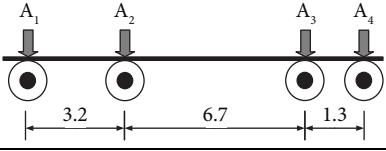
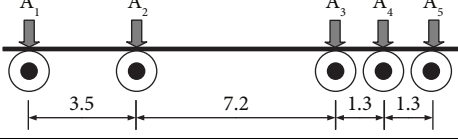
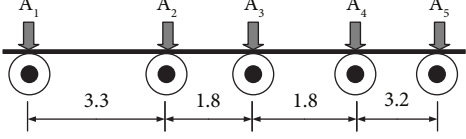
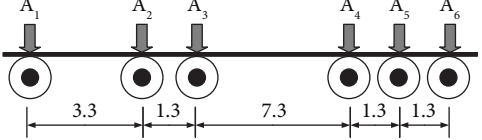
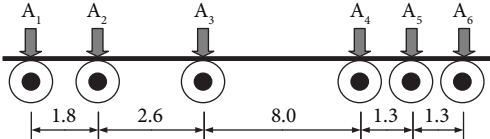
certain type of vehicle is defined in [26] (vehicle load investigation and local fatigue analysis of a highway bridge)

$$A_i = \left[ \sum f_j (A_{ij})^3 \right]^{1/3}, \quad (3)$$

where  $A_{ij}$  is the  $i$ -th axle load of the  $j$ -th car of the representative model.

Figure 8 shows the axle load distribution and corresponding equivalent axle load of each vehicle type. In the «AASHTO LRFD» specifications [27], the standard fatigue car stipulates that the axle load of the front axle is 2.6 t, and the uniaxial axle loads of the middle and rear duplex axles are both 5.4 t. In statistics, the equivalent axle load of most models is too large, and the axle load of the second axle of the V9 model is 17.4 t, which is the largest uniaxial axle load among statistical models. The equivalent axle weight of the V3 rear axle reaches 14.7 t, which shows that the standard fatigue axle weight defined in «AASHTO LRFD» is not applicable. By analysing the distribution characteristics, it can be deduced that the axle load distribution of each vehicle is similar to the mass distribution of the corresponding vehicle, and the axle load of the two-axle vehicle presents a single-peak distribution. For the V3–V11 models, except for the single-peak distribution of the load of the front axle, the multi-peak distribution of the axle load of the rear axle is common. The sum of the equivalent axle load of each vehicle type is consistent with the equivalent mass, and the

TABLE 2: Vehicle model.

Vehicle classification	Vehicle axle count	Amount	The wheelbase
V1	Two-axle	2521	—
V2	Two-axle	873	
V3	Two-axle	1202	
V4	Three-axle	314	
V5	Three-axle	1526	
V6	Four-axle	1152	
V7	Four-axle	1777	
V8	Five-axle	622	
V9	Five-axle	1810	
V10	Six -axle	1441	
V11	Six -axle	368	

difference between them is kept within 1 t. The equivalent vehicle mass can be distributed proportionally to each axle according to the distribution ratio of the vehicle type axle load to obtain the equivalent axle load.

3.4. *Distribution of Vehicle Types in Lanes.* Generally, the traffic lanes of vehicles on the bridge deck are unevenly distributed, which may lead to concentrated areas of fatigue loading. Therefore, it is necessary to study the distribution

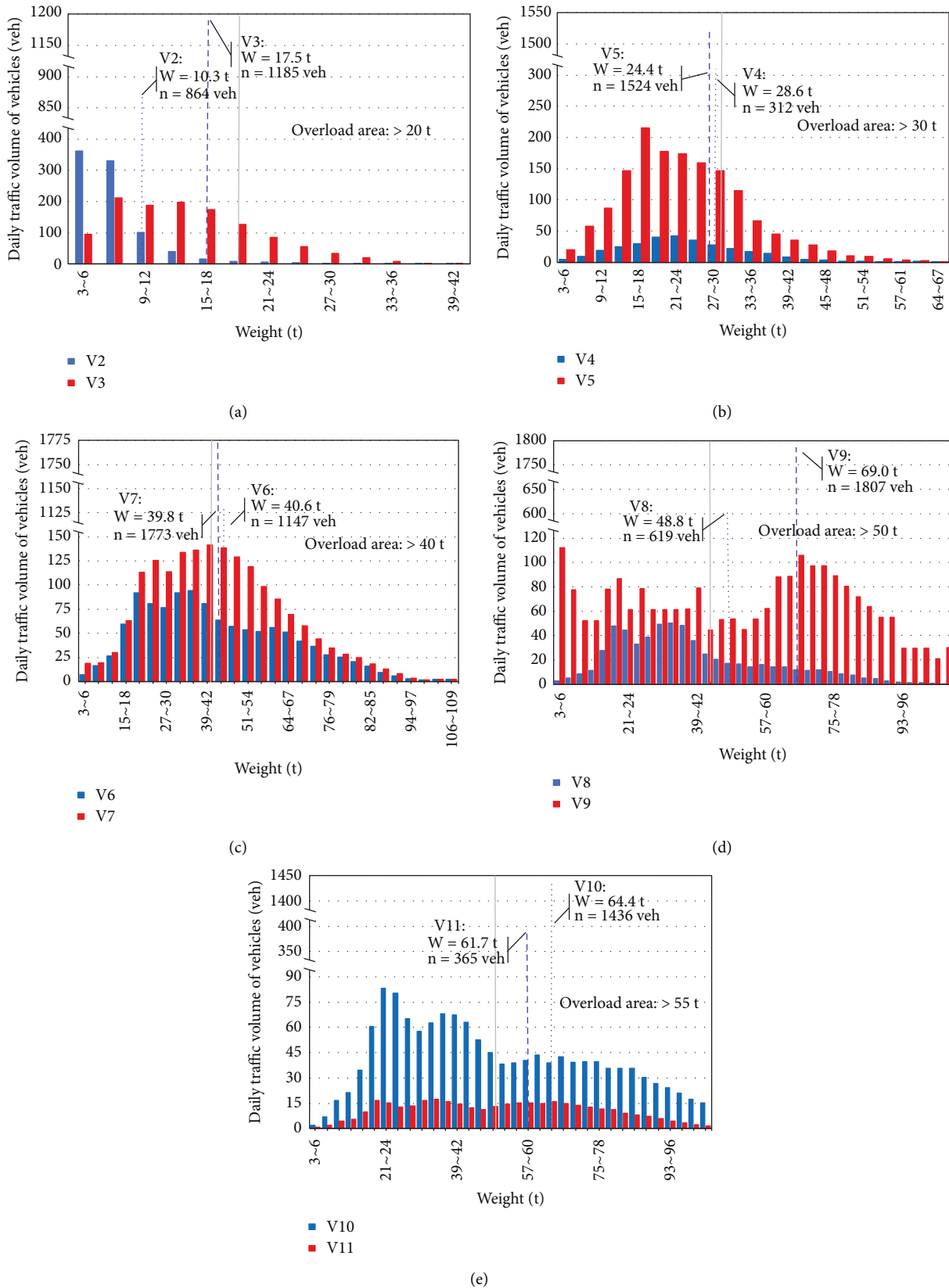


FIGURE 7: Vehicle mass distribution. (a) Mass distributions of representative two-axle and (b) three-axle vehicles, (c) mass distributions of representative four-axle (d) and five-axle vehicles, and (e) mass distributions of representative six-axle vehicles.

TABLE 3: Statistics of overweight vehicles.

Vehicle classification	Overload standard	Number of vehicles	Overloading rate	The biggest quality	Average quality
V2	20	11	1.3	34.7	20.3
V3	20	298	24.8	41.3	23.8
V4	30	101	32.1	60.4	28.6
V5	30	548	35.9	62.3	31.9
V6	40	431	37.4	90.3	43.2
V7	40	759	42.7	83.5	45.9
V8	50	297	47.8	110.6	53.8
V9	50	775	42.8	98.7	64.2
V10	55	984	68.3	134.2	66.8
V11	55	257	69.8	131.1	61.1

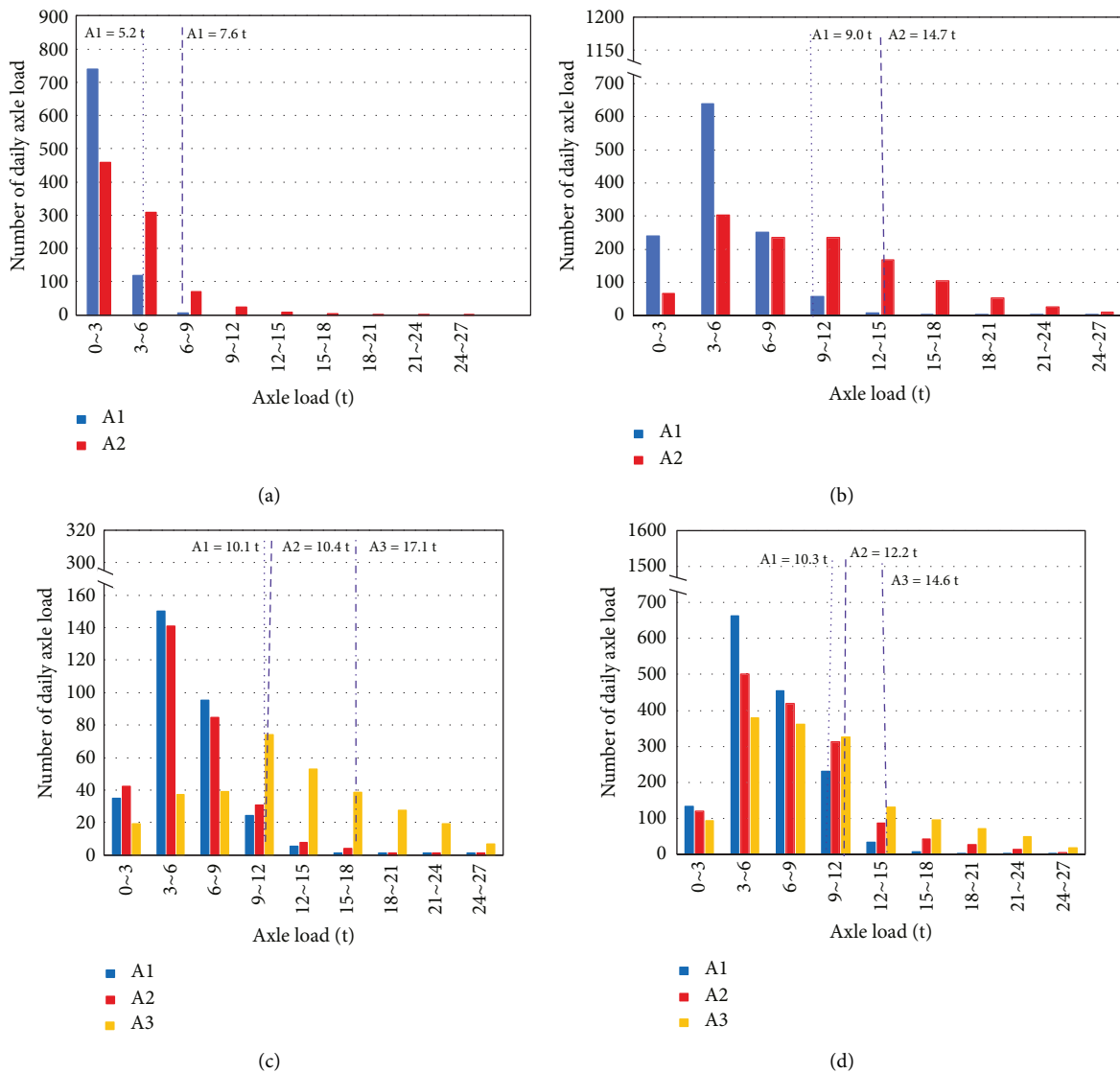


FIGURE 8: Continued.



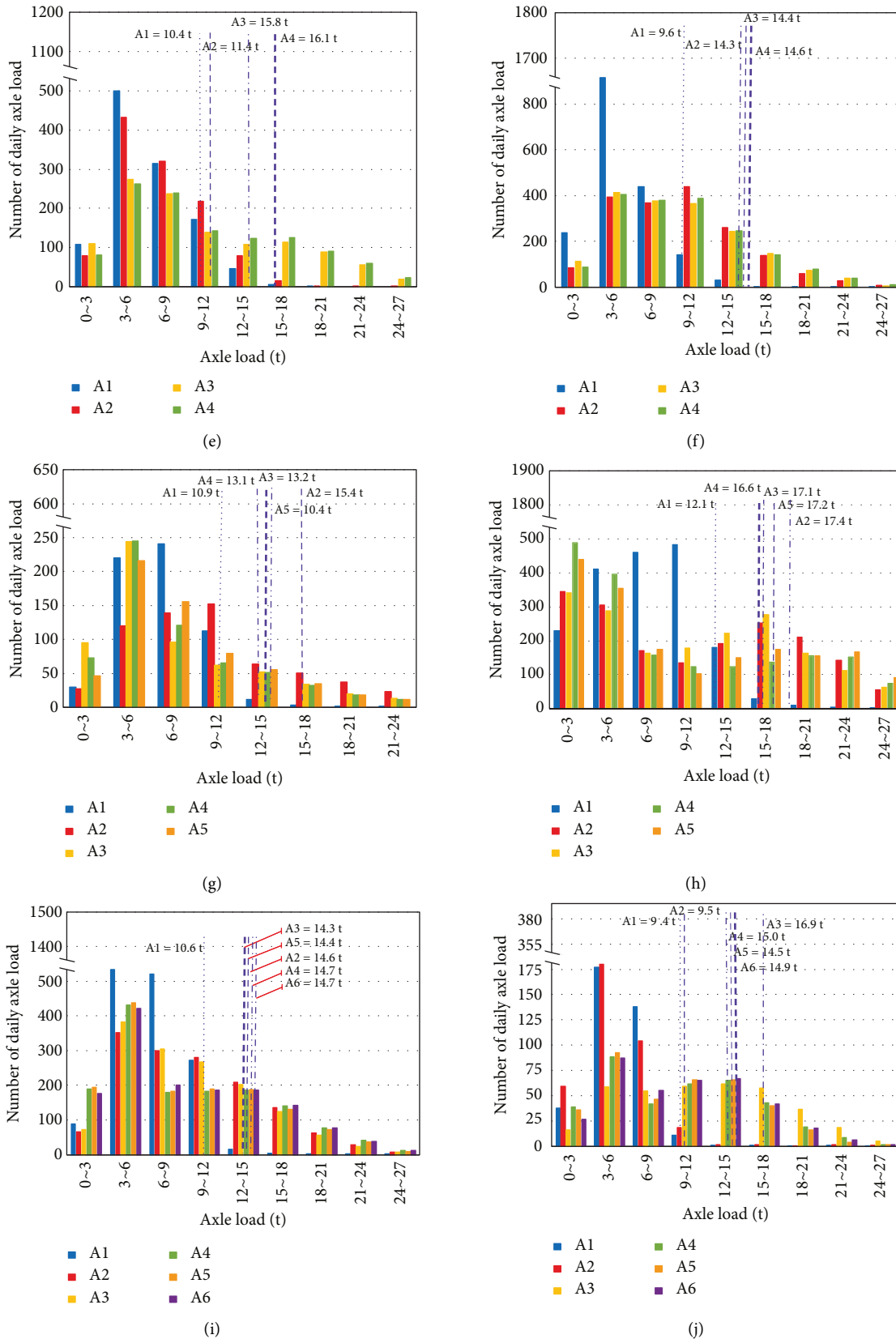


FIGURE 8: Axle load and equivalent axle load of the vehicle. (a) Axle loads and equivalent axle loads of the V2 vehicle type. (b) Axle loads and equivalent axle loads of the V3 vehicle type. (c) Axle loads and equivalent axle loads of the V4 vehicle type. (d) Axle loads and equivalent axle loads of the V5 vehicle type. (e) Axle loads and equivalent axle loads of the V6 vehicle type. (f) Axle loads and equivalent axle loads of the V7 vehicle type. (g) Axle loads and equivalent axle loads of the V8 vehicle type. (h) Axle loads and equivalent axle loads of the V9 vehicle type. (i) Axle loads and equivalent axle loads of the V10 vehicle type. (j) Axle loads and equivalent axle loads of the V11 vehicle type.

TABLE 4: Distribution of representative vehicle types on lanes.

Model	Lane 1		Lane 2		Lane 3		Lane 4		Total	
	Quantity	Proportion (%)	Quantity	Proportion (%)	Quantity	Proportion (%)	Quantity	Proportion (%)	Quantity	Proportion (%)
V1	454	11.38	857	48.78	681	42.35	529	11.73	2521	18.53
V2	192	4.81	244	13.89	210	13.06	227	5.03	873	6.42
V3	301	7.54	276	15.71	325	20.21	301	6.67	1202	8.83
V4	113	2.83	21	1.20	18	1.12	162	3.59	314	2.31
V5	592	14.84	66	3.76	83	5.16	784	17.38	1526	11.22
V6	403	10.10	96	5.46	74	4.60	579	12.84	1152	8.47
V7	843	21.13	87	4.95	99	6.16	783	17.36	1777	13.06
V8	281	7.04	66	3.76	75	4.66	201	4.46	622	4.57
V9	17	0.43	9	0.51	18	1.12	9	0.20	1810	13.30
V10	657	16.47	11	0.63	6	0.37	767	17.00	1441	10.59
V11	137	3.43	24	1.37	19	1.18	169	3.75	368	2.70

characteristics of the vehicle load spectrum along the transverse direction of the bridge. The positions of vehicles on the driving lanes of the bridge are shown in Table 4, where the number in the left column is the proportion of vehicle types to the total traffic flow. The number in the right column is the proportion of vehicle type to the total number of a vehicles of the same type. Generally, V2–V11 models account for 81.5% of the total traffic flow. Although the number of V2 vehicles is large, their contribution to fatigue damage is negligible owing to the small vehicle mass. Although V3 is a two-axle vehicle, its influence on bridge-fatigue load cannot be ignored because of the significant overload and large body mass.

**3.5. Axle Redistribution of Lanes.** The distribution of vehicles in different positions across the bridge results in different dynamic load effects on the bridge structure. By statistically analysing the distribution law of the lateral position of the traffic flow, the traffic flow can be simulated more accurately, thereby obtaining an analysis and calculation of the bridge structure closer to the actual situation. Figure 9 shows the axle load distribution of each lane according to the vehicle load spectrum. The vehicles running in lanes 2 and 3 are mainly two-axle vehicles; therefore, the equivalent axle load is small. The traffic volume in lanes 1 and 4 is considerable, and the load imbalance of the lanes in the same direction is significant, which is extremely unfavourable to the fatigue performance of CFST arch bridges, especially the suspenders of the arch bridges.

## 4. Fatigue Vehicle Model

**4.1. Standard Fatigue Vehicle Model.** Based on the principle of fatigue damage equivalence, the representative vehicle model that has the greatest influence on bridge-fatigue loading can be obtained through the vehicle load spectrum, and a fatigue vehicle model can be proposed by taking this vehicle model as the prototype. The fatigue loading contribution is defined as

$$C_k = \frac{r_k W_k^3}{\sum_{k=1}^N r_k W_k^3}, \quad (4)$$

where  $C_k$  contributes to the fatigue loading of representative vehicle type  $K$ ,  $r_k$  is the frequency of the representative

vehicle in the traffic flow,  $W_k$  is the equivalent mass of representative vehicle type  $K$ , and  $N$  represents the vehicle type.

Table 5 presents the fatigue contribution of each representative vehicle in the vehicle load spectrum. From the table, it can be observed that the number of vehicles and the vehicle type have little influence on the fatigue load contribution, and the main factor that affects the fatigue load contribution is the vehicle mass. V2 traffic frequency accounts for 9.35% of the total traffic rate, but because the equivalent vehicle mass of this vehicle is 10.3 t, its contribution to fatigue loading is only 0.14%. The traffic volume of V3 two-axle trucks is equal to that of V2, but the equivalent mass of V3 reached 22.2 t, and the contribution rate to fatigue reached 1.95%, which shows that the contribution of two-axle trucks to the bridge-fatigue load cannot be ignored. The loading contribution of three-axle cars (V4 and V5) is 0.67% and 3.17%, the loading contribution of four-axle cars (V6 and V7) is 5.87% and 15.40%, and the loading contribution of five-axle cars (V8 and V9) is 10.73% and 1.04%, respectively. The fatigue loading contribution of the V10 model is 49.46%, which is the largest among all models. The fatigue loading contribution of the V11 model is 11.56%. According to the vehicle load spectrum and fatigue contribution, the V10 model with the largest fatigue contribution can be used as a prototype vehicle for the fatigue vehicle. Subsequently, according to the load characteristics of the V10 model, the fatigue vehicle model and simplified fatigue vehicle model suitable for this bridge can be derived.

The load effect research of suspenders and other bridge components of an arch bridge will depend on the fatigue vehicle model. To facilitate the application of the fatigue vehicle model, except for the axle load of the first axle, the axle load of the other axles of the vehicle model is equally distributed in this paper, as shown in Figure 10. This simplified method brings very small errors in practical application. To have a better comparison, Figure 11 shows the standard fatigue vehicle model defined by «AASHTO LRFD». The recommended fatigued vehicle model can be transformed into a simplified fatigued vehicle model using a treatment similar to the «AASHTO LRFD» specification. The adjacent axles of the prototype vehicle were merged into

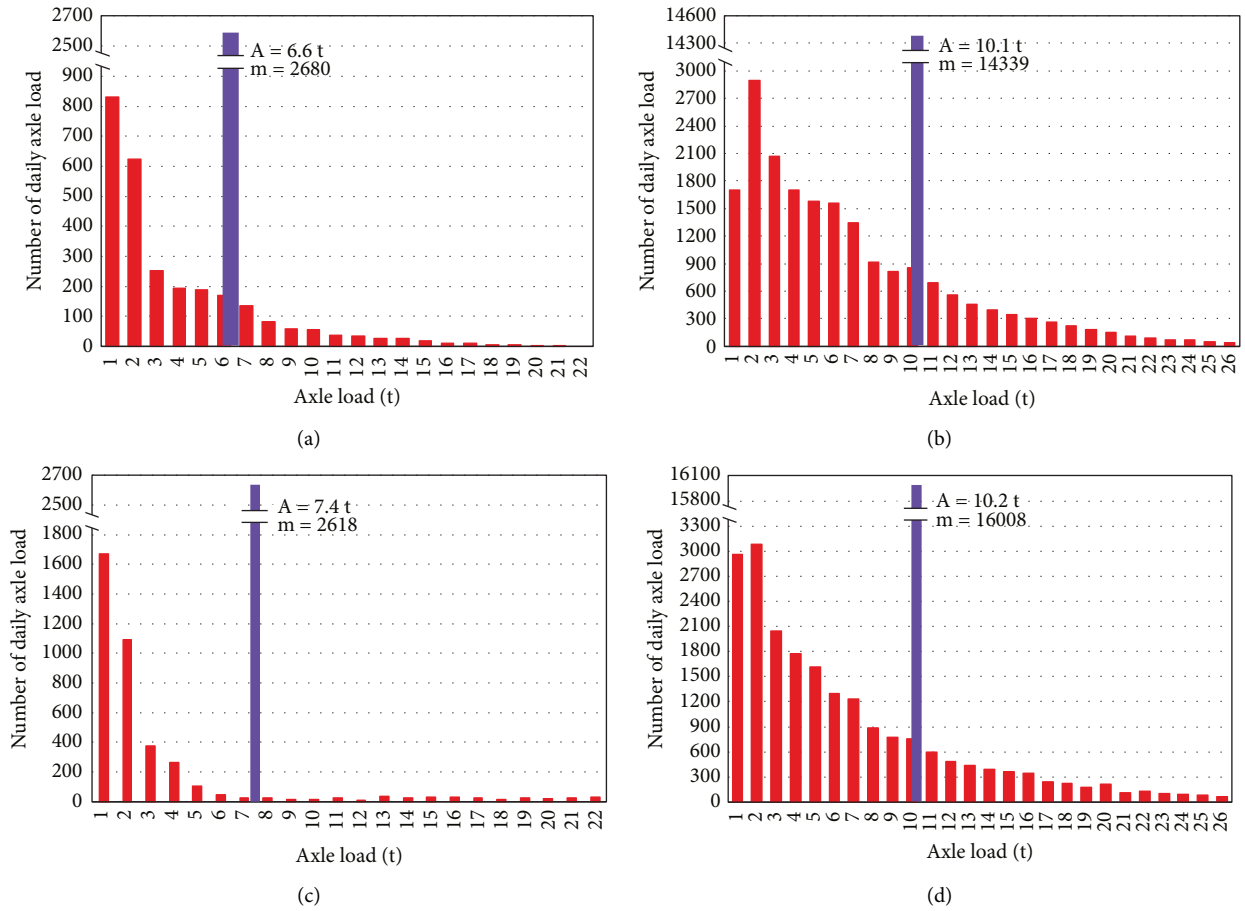


FIGURE 9: Axle load distribution and equivalent axle load. (a) Lane 1. (b) Lane 2. (c) Lane 3. (d) Lane 4.

TABLE 5: Vehicular load spectra and fatigue loading contribution.

Model	Vehicle weight	Quantity	Fatigue vehicle load spectrum	
			Frequency (%)	Loading contribution rate (%)
V2	10.3	872	9.35	0.14
V3	22.2	1202	12.89	1.95
V4	24.3	314	3.37	0.67
V5	24.1	1526	16.36	3.17
V6	32.5	1152	12.35	5.87
V7	38.8	1777	19.05	15.40
V8	48.8	622	6.67	10.73
V9	51	53	0.57	1.04
V10	61.4	1440	15.44	49.46
V11	59.6	368	3.95	11.56

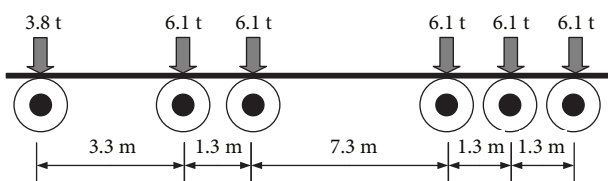


FIGURE 10: Suggested fatigue truck model.

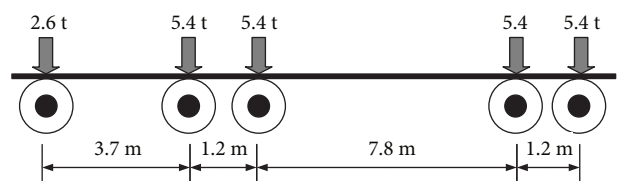


FIGURE 11: Standard fatigue truck model of AASHTO LRFD.

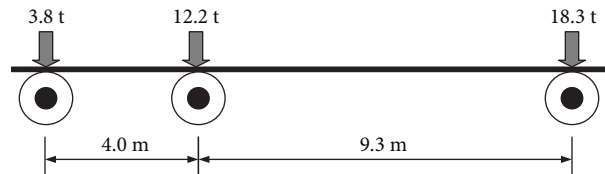


FIGURE 12: Suggested simplified fatigue truck model.

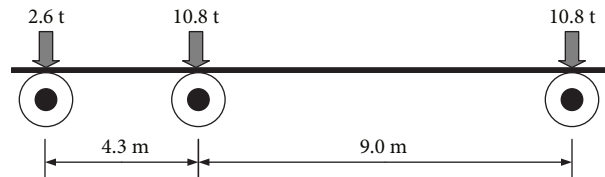


FIGURE 13: Simplified standard fatigue truck model of AASHTO LRFD.

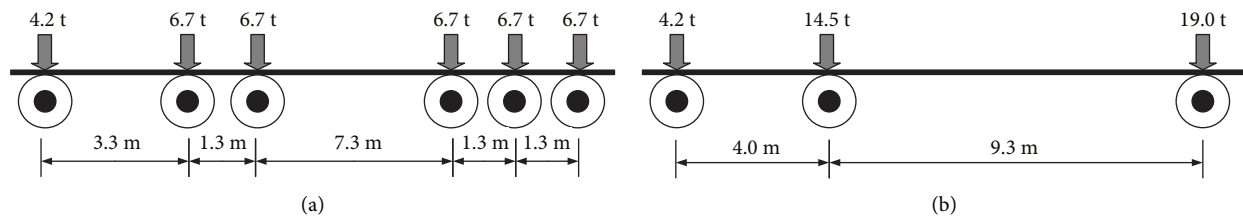


FIGURE 14: Suggested fatigue truck models. (a) Fatigue vehicle model. (b) Simplified fatigue vehicle model.

one axle, and the merged axle was located at the center line of the previous adjacent axles as a method to simplify the model.

By comparing Figures 12 and 13, it can be seen that although the uniaxial axle load of the standard fatigue vehicle model suggested in this paper is close to that of «AASHTO LRFD», the rear axle of the fatigue vehicle proposed in this paper is a three-axle type, and the simplified fatigue vehicle model obtained has a rear axle load of 18.25 t, which is significantly higher than the simplified fatigue vehicle rear axle load of 10.8 t in the AASHTO LRFD. In addition, the fatigue vehicle mass recommended in this paper is 34.3 t, which is also significantly larger than the fatigue vehicle mass of 24.2 t recommended by AASHTO LRFD.

**4.2. Fatigue Vehicle Model of Heavy-Duty Lane.** AASHTO LRFD suggests that the daily average truck traffic volume of one lane should be used for fatigue design. The short suspenders of arch bridges are more severely affected by the vehicle load. According to a previous statistical analysis, the distribution of trucks on the bridge deck is uneven, and 71.6% of the trucks are distributed near the suspenders, especially in the No. 4 lane. To evaluate the fatigue performance of the suspender under the action of heavy vehicles more reasonably, it is necessary to deduce the standard fatigue vehicle and simplified fatigue vehicle models corresponding to the lane near the suspender according to the aforementioned data of vehicle mass and axle load distribution in the lane.

Figure 14 shows the recommended fatigue truck model. Compared with the one-way standard fatigue and simplified fatigue vehicle models derived above, the standard fatigue vehicle model of the heavy-duty lane and the simplified fatigue vehicle model derived in this paper have the same wheelbase distribution, but all axle loads have increased, and the fatigue vehicle mass has increased to 37.7 t, which is approximately 10% larger than the one-way standard fatigue vehicle mass proposed in this paper and approximately 1.6 times larger than the AASHTO LRFD standard fatigue vehicle mass. This is a further indication that the highway has a large traffic volume of trucks, a high proportion of trucks, and significant overload.

## 5. Conclusion

In this paper, the vehicle load of a long-span concrete-filled steel tube arch bridge was calculated and statistically based on WIN system data. The vehicle type, axle load, axle base, and load distribution were taken into consideration, and the vehicle load spectrum and vehicle model in accordance with the real local vehicle traffic state were obtained by analysis and calculation, and compared with «AASHTO LRFD» specification. The main conclusions are as follows:

- (1) The fatigue vehicle load spectrum can be classified into 10 representative models. The vehicle distribution and axle load distribution along the lane were given based on the corresponding wheelbase, vehicle mass, axle load, and overload data, and the six-axis

V10 model was determined to be the vehicle with the largest contribution rate to fatigue load.

- (2) The freight cars passing on the CFST arch bridge have a large load, and the proportion of freight cars in the total traffic flow is larger. The total mass and axle load of freight cars are significantly overloaded, and the load is concentrated near the suspender lane. Lanes 1 and 4 together account for 70 percent of the vehicles.
- (3) «AASHTO LRFD» defines a truck that causes fatigue damage to a bridge as a vehicle with more than two axles. Because the weight and axle load of an overloaded two-axle vehicle may be relatively large, the influence of the two-axle truck on fatigue loading cannot be ignored.
- (4) The fatigue vehicle models and corresponding simplified models of ordinary and heavy-duty vehicles with vehicle masses of 34.3 t and 37.7 t, respectively, were proposed. The common fatigue car model is 10.1 t heavier than the fatigue car model suggested in the AASHTO specification.
- (5) The fatigue vehicle model of the long-span CFST arch bridge proposed in this paper has a specific region, which leads to a certain limitation in the application scope of the model.

## Data Availability

The raw/processed data required to reproduce these findings cannot be shared at this time as the data also form part of an ongoing study.

## Conflicts of Interest

The authors declare that they do not have any commercial or associative interest that represents conflicts of interest in connection with the work submitted.

## Acknowledgments

This work was supported by the National Nature Science Foundation of China (Grant nos. 51678459 and 51378406) and the Technology Project of Shanxi Transportation Holdings Group Co., Ltd. (Grant No. 19-JKKJ-8).

## References

- [1] G. Fu and O. Hag-Elsafi, "Vehicular overloads: load model, bridge safety, and permit checking," *Journal of Bridge Engineering*, vol. 5, no. 1, pp. 49–57, 2000.
- [2] Z. Zhiwen, H. Yan, and X. Ze, "Fatigue performance of floorbeam cutout detail of orthotropic steel bridge on heavy freight transportation highway," *China Journal of Highway and Transport*, vol. 30, no. 3, pp. 104–112, 2017.
- [3] P. Peng, L. Quanwang, and E. A. Zhou Yibin, "Vehicle survey and local fatigue analysis of a highway bridge," *China Civil Engineering Journal*, vol. 44, no. 5, pp. 94–100, 2011.
- [4] P. Chotickai and M. D. Bowman, "Truck models for improved fatigue life predictions of steel bridges," *Journal of Bridge Engineering*, vol. 11, no. 1, pp. 71–80, 2006.
- [5] S. W. Haider and R. S. Harichandran, "Relating axle load spectra to truck gross vehicle weights and volumes: proceedings of the American Society of Civil Engineers," *Journal of Transportation Engineering*, vol. 133, no. 12, pp. 696–705, 2007.
- [6] J. A. Laman and A. S. Nowak, "Fatigue-load models for girder bridges," *Journal of Structural Engineering*, vol. 122, no. 7, pp. 726–733, 1996.
- [7] H. Cohen, G. Fu, W. Dekelbab, and F. Moses, "Predicting truck load spectra under weight limit changes and its application to steel bridge fatigue assessment," *Journal of Bridge Engineering*, vol. 8, no. 5, pp. 312–322, 2003.
- [8] E. J. O'Brien, B. Enright, and A. Getachew, "Importance of the tail in truck weight Modeling for bridge assessment," *Journal of Bridge Engineering*, vol. 15, no. 2, pp. 210–213, 2010.
- [9] J. Zhao and H. Tabatabai, "Evaluation of a permit vehicle model using weigh-in-motion truck records," *Journal of Bridge Engineering*, vol. 17, no. 2, pp. 389–392, 2012.
- [10] G. Fiorillo and M. Ghosn, "Procedure for statistical categorization of overweight vehicles in a WIM database," *Journal of Transportation Engineering*, vol. 140, no. 5, Article ID 4014011, 2014.
- [11] C. Leahy, E. J. O'Brien, B. Enright, and D. Hajjalizadeh, "Review of HL-93 bridge traffic load model using an extensive WIM database," *Journal of Bridge Engineering*, vol. 20, no. 10, pp. 1–8, 2015.
- [12] W. S. Han, J. Wu, C. S. Cai, and S. Chen, "Characteristics and dynamic impact of overloaded extra heavy trucks on typical highway bridges," *Journal of Bridge Engineering*, vol. 20, no. 2, p. 1, 2015.
- [13] Z. Yongtao, B. Weigang, Z. Hui, and Y. Liu, "Study of standard fatigue design load for steel highway bridge," *China Civil Engineering Journal*, vol. 1, pp. 79–85, 2010.
- [14] C. Lan, H. Li, and J. Ou, "Traffic load modelling based on structural health monitoring data," *Structure and Infrastructure Engineering*, vol. 7, no. 5, pp. 379–386, 2011.
- [15] N. W. Lu, M. Noori, and Y. Liu, "Fatigue reliability assessment of welded steel bridge decks under stochastic truck loads via machine learning," *Journal of Bridge Engineering*, vol. 22, no. 1, pp. 1–12, 2017.
- [16] Z. Zhang, H. Wang, T. Yang, L. Wang, and X. Wang, "Fatigue durability analysis for suspenders of arch bridge subjected to moving vehicles in southwest China," *Sustainability*, vol. 14, no. 16, p. 10008, 2022.
- [17] B. Chen, X. Li, X. Xie, Z. Zhong, and P. Lu, "Fatigue performance assessment of composite arch bridge suspenders based on actual vehicle loads," *Shock and Vibration*, vol. 2015, Article ID 659092, 13 pages, 2015.
- [18] H. Sun, J. Ma, and B. Yu, "Study on suspender's fatigue performance of half-through CFST arch bridge due to vehicular loads," *Advanced Engineering Forum*, vol. 5, pp. 189–194, 2012.
- [19] L. Xinxing, R. Weixin, and Z. Jiwei, "Standard fatigue truck on montane speedway bridge," *Journal of Vibration and Shock*, vol. 31, no. 15, pp. 96–100, 2012.

- [20] X. Yefei, L. Fengfeng, and E. A. Gu Yu, "Study on vehicular fatigue load spectrum expressway bridge based on WIN system," *Journal of Highway and Transportation Research and Development*, vol. 3, pp. 56–64, 2014.
- [21] L. Songhui, X. Zhongyan, and J. Hanwan, "Influence of overweight vehicles on bridge safety," *Journal of Highway and Transportation Research and Development*, vol. 32, no. 9, pp. 74–79, 2015.
- [22] Y. Deng and L. Deng, "Suspender replacement method for long-span concrete-filled steel tubular arch bridges and cable force measurement based on frequency method," *Advances in Civil Engineering*, vol. 202121 pages, Article ID 7308816, 2021.
- [23] Z. Zhu and Z. Xiang, "Fatigue cracking investigation on diaphragm cutout in a self-anchored suspension bridge with orthotropic steel deck," *Structure and Infrastructure Engineering*, vol. 15, no. 10, pp. 1279–1291, 2019.
- [24] Z. Zhu, Z. Xiang, J. L. J. Li, and A. Carpinteri, "Fatigue damage investigation on diaphragm cutout detail on orthotropic bridge deck based on field measurement and FEM," *Thin-Walled Structures*, vol. 157, Article ID 107106, 2020.
- [25] X. Shao, D. Yi, Z. Huang, H. Zhao, B. Chen, and M. Liu, "Basic performance of the composite deck system composed of orthotropic steel deck and ultrathin RPC layer," *Journal of Bridge Engineering*, vol. 18, no. 5, pp. 417–428, 2013.
- [26] W. Chang, W. Yuzhu, and C. Bing, "Experiment on effect of stress ratio on out-of-plane distortion-induced fatigue performance of web gaps in steel bridges," *China Journal of Highway and Transport*, vol. 30, no. 3, pp. 72–81, 2017.
- [27] A. Lrfd, *AASHTO LRFD Bridge Design Specifications*, American Association of State Highway Transportation Officials, Washington DC, 2004.